Available online at www.sciencedirect.com

SciVerse ScienceDirect

Ceramics International 38 (2012) 5691–5697

CERAMICS INTERNATIONAL

www.elsevier.com/locate/ceramint

Formation of chromium borides by combustion synthesis involving borothermic and aluminothermic reduction of Cr_2O_3

C.L. Yeh *, J.Z. Lin, H.J. Wang

Department of Aerospace and Systems Engineering, Feng Chia University, 100 Wenhwa Rd., Seatwen, Taichung 40724, Taiwan

Received 13 March 2012; received in revised form 3 April 2012; accepted 3 April 2012
Available online 12 April 2012

Abstract

Chromium borides of various phases were fabricated through combustion synthesis in the mode of self-propagating high-temperature synthesis (SHS) by adopting the powder compacts of $Cr_2O_3 + xB$ (with $x = 4$–9) and $Cr_2O_3 + 2Al + yB$ (with $y = 1$–8). Because aluminothermic reduction of Cr_2O_3 is more exothermic than borothermic reduction, the reaction temperature and combustion front velocity of the Al-added samples are much higher than those of the Cr_2O_3–B samples. In agreement with the composition dependence of reaction exothermicity, the fastest combustion wave was observed in the compact with $x = 6$ for the Cr_2O_3–B sample and $y = 4$ for the Cr_2O_3–Al–B sample. According to the XRD analysis, Cr_5B_3, CrB, and CrB_2 were produced in the monolithic form respectively from the Cr_2O_3–B samples of $x = 4$, 5, and 9, or in the composite form from samples of other stoichiometries. On the other hand, five different borides were identified in Al_2O_3-added products. Among them, Cr_2B, CrB, and CrB_2 were yielded as the sole boride compound from the Al-added samples of $y = 1.2$, 3, and 7 or 8, respectively. Cr_5B_3 and Cr_3B_4 were produced along with CrB as the secondary phase. Based upon experimental evidence, it was found that an excess amount of boron in the reactant mixture was required to facilitate the formation of chromium borides.

Keywords: Chromium borides; Self-propagating high-temperature synthesis (SHS); Reduction reaction; X-ray diffraction

1. Introduction

It has been well recognized that combination of their high melting point, high hardness, good electrical and thermal conductivity, chemical inertness, and excellent wear and corrosion resistance makes transition metal borides, such as TiB_2, ZrB_2, HfB_2, and TaB_2, potential candidates for high-temperature structural applications [1,2]. So far, a variety of transition metal borides have been produced from their constituent elements through combustion synthesis in the mode of self-propagating high-temperature synthesis (SHS) [3–7]. However, when direct combustion between the metal and boron is not feasible due largely to insufficient exothermicity, the SHS process involving borothermic reduction of metal oxides has been considered as an alternative of preparing the corresponding metal borides [8–10]. Metallic elements of the IVB and VB groups are members of the former, while those of the VIB group (Cr, Mo, and W) belong to the latter. Consequently, molybdenum borides (Mo_2B, MoB_2, and Mo_2B_5) were produced from the SHS process simultaneously involving borothermic reduction of MoO_3 and elemental interaction between Mo and boron [9]. Likewise, tungsten borides (WB and W_2B_5) were fabricated from self-sustaining combustion of the powder compacts composed of WO_3, W, and boron [10]. Nevertheless, available literature on the preparation of chromium borides by combustion in the self-propagating mode is very limited.

For the Cr–B system, six chromium borides (Cr_2B, Cr_5B_3, CrB, Cr_3B_4, CrB_2, and CrB_4) shown in Fig. 1 have been reported [11]. Among them, CrB_2 is the most stable compound with a melting point of 2200 °C and is a potential candidate as the structural material, hard coating on cutting tools, and protective layer on mechanical parts to resist wear and corrosion [12,13]. As an additive, CrB_2 improves the mechanical and electrical properties and oxidation resistance of B_4C [14,15]. On the preparation of chromium borides, CrB_2 has been the most produced phase. Iizumi et al. [16] obtained CrB and CrB_2 in pure form by milling chromium and boron

* Corresponding author. Tel.: +886 4 24517250x3963; fax: +886 4 24510862.
E-mail address: clyeh@fcu.edu.tw (C.L. Yeh).

0272-8842/$36.00
http://dx.doi.org/10.1016/j.ceramint.2012.04.013

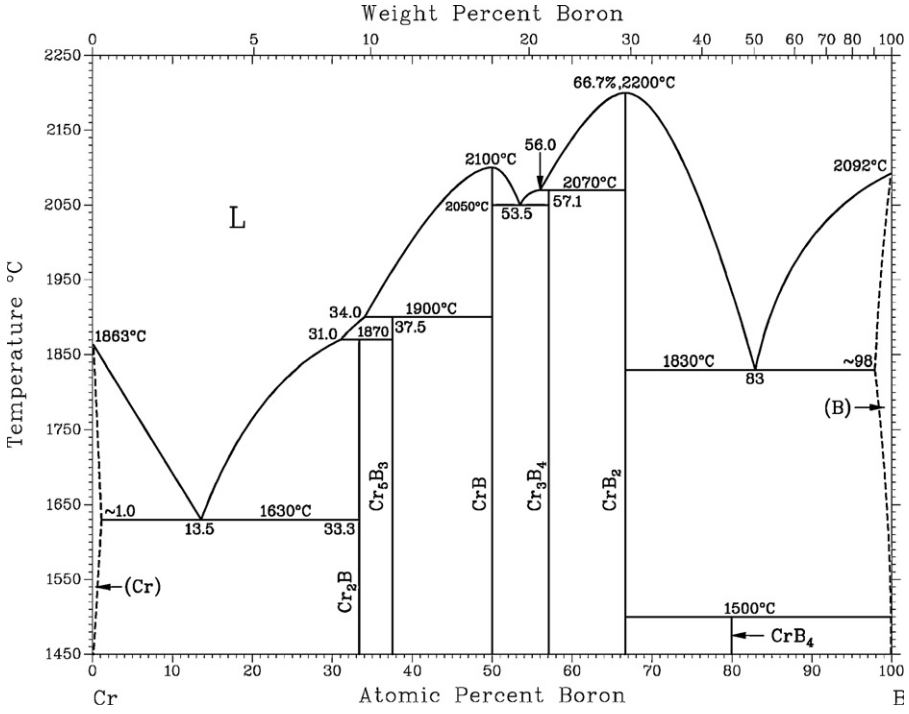

Fig. 1. Phase diagram of Cr–B binary system [11].

powders in a planetary ball mill for 20–40 h, followed by annealing at 900–1000 °C for 2 h. Peshev et al. [17] conducted borothermic reduction of Cr_2O_3 at 1600 °C to produce CrB_2. Through self-propagating combustion involving reduction of Cr_2O_3 by amorphous boron, Yeh and Wang [18] fabricated three chromium borides, Cr_5B_3, CrB, and CrB_2, in either monolithic or composite form from powder compacts with different molar ratios of B/Cr_2O_3. As reported by Sonber et al. [19], CrB_2 was synthesized through reduction of Cr_2O_3 by B_4C in the presence of carbon at 1700 °C for 2 h. The optimum sample composition for the formation of single-phase CrB_2 was found to be Cr_2O_3:B_4C:C = 1:1.2:1.31, which contained excess boron to compensate for the loss of boron as B_2O_3 evaporated [19].

In contrast to the aforementioned time-consuming and energy-intensive methods, the SHS process takes advantage of the self-sustaining merit from exothermic reactions and hence has the potential of time and energy savings [20]. However, self-sustaining combustion cannot be achieved for an elemental Cr–B powder compact due to weak exothermicity. Therefore, this study attempts to incorporate the borothermic and aluminothermic reduction of Cr_2O_3 into the synthesis reaction of chromium borides. Such a fabrication route aims at gaining a benefit from the large reaction enthalpy of metallothermic reduction of Cr_2O_3 to facilitate combustion synthesis in the SHS manner. When Al is adopted as the reducing agent, the synthesis reaction represents an in situ procedure of preparing Al_2O_3-reinforced materials and has been applied to produce composites, like TiB_2–Al_2O_3, ZrB_2–Al_2O_3, TiC–Al_2O_3, TiAl–Al_2O_3, etc. [21–24]. The addition of Al_2O_3 was shown to improve the fracture toughness, flexural strength, and impact resistance of the composite [23–26]. The specific objective of this study is to conduct a comparison between the SHS processes involving borothermic and aluminothermic reduction of Cr_2O_3. Not only are chromium borides formed from combustion investigated, but also combustion characteristics are explored, including the sustainability of combustion, flame-front velocity, and combustion temperature.

2. Experimental methods of approach

Chromium oxide Cr_2O_3 (Showa Chemical Co., 99% purity), amorphous boron (Noah Technologies Corp., 92% purity), and Al (Showa Chemical Co., <45 μm, 99.9%) powders were employed as the starting materials to prepare two types of the powder mixtures. One is composed of Cr_2O_3 and boron with a molar composition of $Cr_2O_3 + xB$. The value of the parameter x ranges between 3 and 10 for covering the entire stoichiometry of six chromium borides. The other type of the sample adopts Al as the reducing agent and is formulated by the molar proportion of $Cr_2O_3 + 2Al + yB$ with y = 1–8. The synthesis process of the Cr_2O_3–B sample essentially combines the reduction of Cr_2O_3 by B to form elemental Cr and B_2O_3 as a by-product and the interaction between the reduced Cr and B to yield boride compounds. On the other hand, chromium borides are produced along with Al_2O_3 from the samples containing Cr_2O_3, Al, and B powders. The following reactions are two examples of the formation of CrB and CrB_2 from stoichiometric Cr_2O_3–B and Cr_2O_3–Al–B samples, respectively.

$$Cr_2O_3 + 4B \rightarrow 2CrB + B_2O_3 \quad (1)$$

$$Cr_2O_3 + 2Al + 4B \rightarrow 2CrB_2 + Al_2O_3 \quad (2)$$

The reactant powders with a prescribed composition were dry mixed in a ball mill and then cold-pressed into cylindrical

test specimens with a diameter of 7 mm, a height of 12 mm, and a compaction density relative to 45% of the theoretical maximum density (TMD). The SHS experiment was conducted in a stainless-steel windowed chamber under an atmosphere of high-purity argon (99.99%). The sample holder is equipped with a 600 W cartridge heater used to raise the initial temperature of the sample prior to ignition. Details of the experimental setup and measurement approach were reported elsewhere [27]. It was found that in order to achieve self-sustaining combustion, the preheating temperatures (T_p) of 300 and 200 °C were respectively required for the Cr_2O_3–B and Cr_2O_3–Al–B samples. Besides, the Cr_2O_3–B sample needs a Ti–C pellet with an atomic ratio of Ti:C = 1:1 placed on its upper plane to serve as an ignition enhancer which is triggered by a heated tungsten coil. A lower preheating temperature and no need of an ignition enhancer for the Cr_2O_3–Al–B sample suggest that the SHS process involving reduction of Cr_2O_3 by Al is more exothermic and easier to proceed than that based upon borothermic reduction of Cr_2O_3. According to the thermochemical data from Ref. [28], the reaction heat (ΔH_r) per one mole of the product formed and adiabatic temperature (T_{ad}) of the displacement reaction of Cr_2O_3 with Al (i.e., $1/3Cr_2O_3 + 2/3Al \rightarrow 2/3Cr + 1/3Al_2O_3$) are −180.3 kJ/mol and 2164 K, respectively. However, both ΔH_r (=−45.7 kJ/mol) and T_{ad} (=1257 K) are much lower for borothermic reduction of Cr_2O_3.

3. Results and discussion

3.1. Observation of combustion characteristics

Fig. 2(a) and (b) illustrates typical SHS sequences associated with solid-state combustion of the Cr_2O_3–B and Cr_2O_3–Al–B powder compacts, respectively. It is evident that the distinct and nearly parallel combustion front forms upon ignition and propagates along the sample in a self-sustaining manner. For the powder compact of Cr_2O_3:B = 1:5 shown in Fig. 2(a), the combustion wave traverses the entire sample in about 5.20 s and accompanies a shrinkage of the burned sample. It is believed that formation of molten B_2O_3 (with a low melting point of 460 °C) during combustion causes contraction of the sample and subsequent densification of the final product. When compared with those observed in Fig. 2(a), a brighter burning glow and a faster combustion front are noticed in Fig. 2(b) for combustion of an Al-added sample with stoichiometry of Cr_2O_3:Al:B = 1:2:3. This is due most likely to the greater exothermicity for reduction of Cr_2O_3 by Al than that by boron. However, the Al-added compact experienced a less degree of

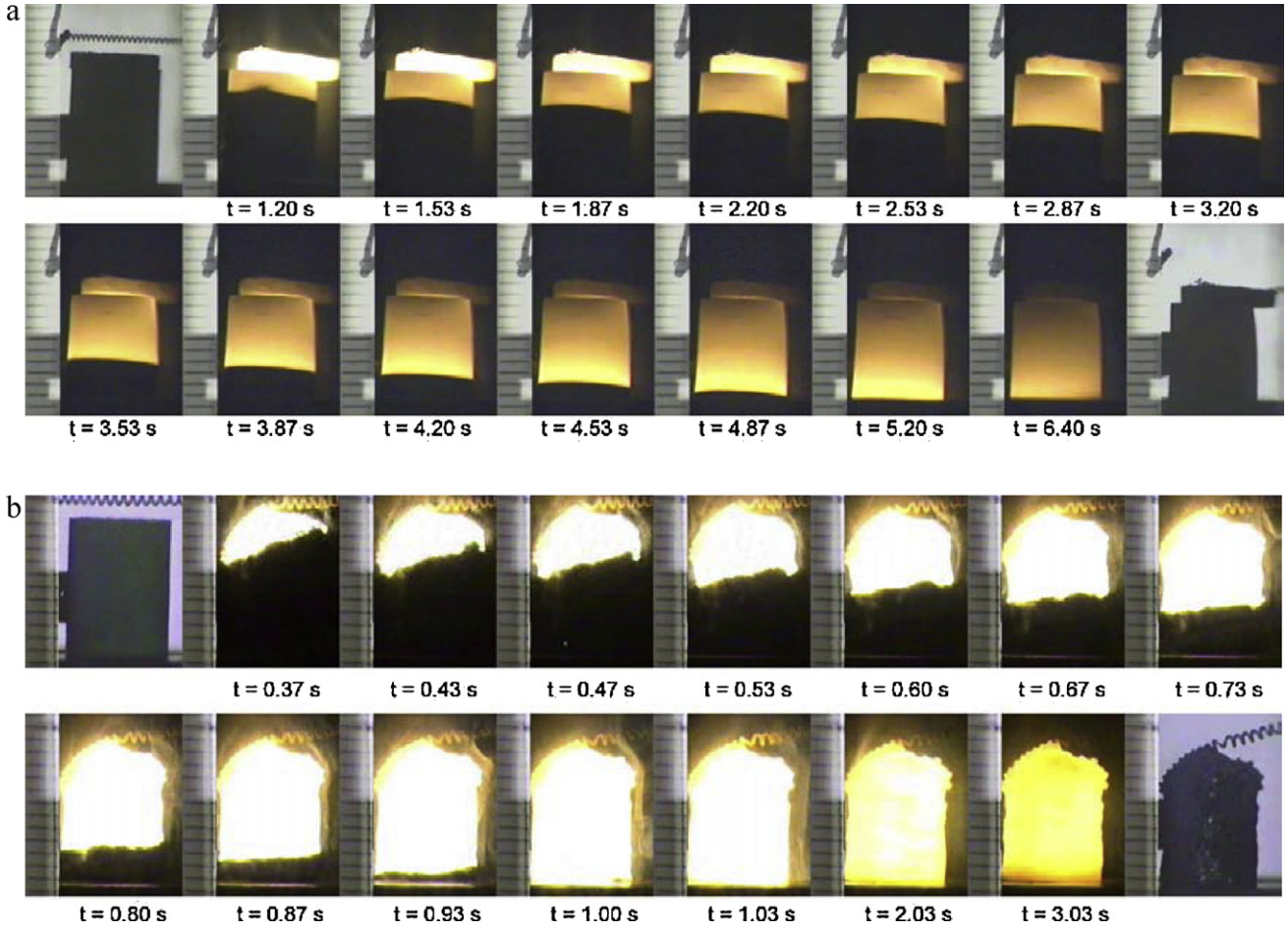

Fig. 2. Recorded SHS sequences illustrating self-sustaining propagation of combustion along powder compacts with molar proportions of (a) Cr_2O_3:B = 1:5 and (b) Cr_2O_3:Al:B = 1:2:3.

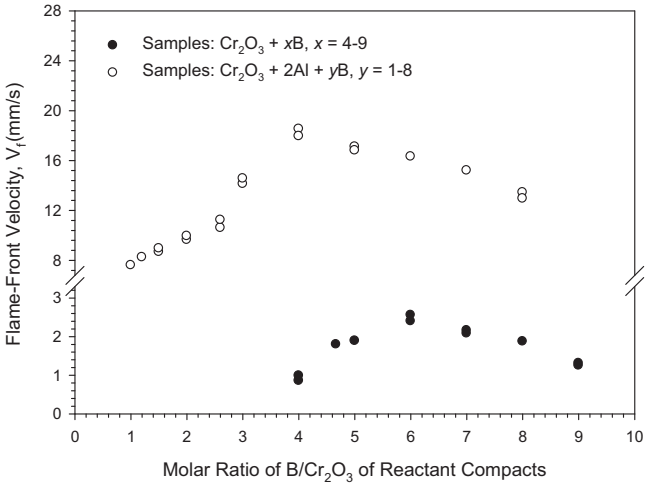

Fig. 3. Effect of molar ratio of B/Cr_2O_3 on flame-front propagation velocity of Cr_2O_3–B and Cr_2O_3–Al–B powder compacts.

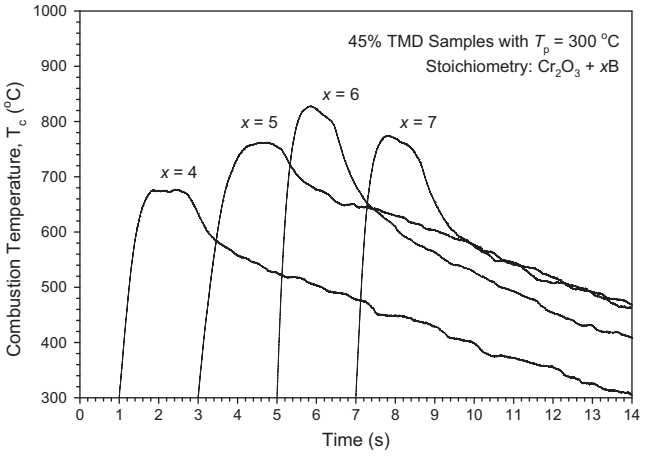

Fig. 4. Effect of boron content on combustion temperature of powder compacts with stoichiometry of Cr_2O_3 + xB.

the sample shrinkage during combustion, since the by-product formed was Al_2O_3 rather than B_2O_3.

3.2. Measurement of flame-front propagation velocity

The propagation velocity (V_f) of the combustion front was determined from recorded SHS images. As presented in Fig. 3, the flame-front velocity is significantly affected by the molar ratio of B/Cr_2O_3 of the reactant mixture and by the substitution of Al for boron as the reducing agent. Although the samples of Cr_2O_3 + xB with x = 3–10 were conducted in this study, the experimental observation indicated a stoichiometric range for self-sustaining combustion residing in $4 \leq x \leq 9$, beyond which combustion ceased to propagate and quenched. This implies a lack of sufficient reaction exothermicity for the Cr_2O_3–B samples with x = 3 and 10. Moreover, as shown in Fig. 3, there exists a sample composition under which the combustion wave velocity reaches a maximum. Namely, with the increase of the boron content from x = 4 to 9, the combustion wave velocity increases from 0.86 mm/s to a peak value of 2.56 mm/s at x = 6, and then decreases to about 1.25 mm/s for the compact containing boron at x = 9.

On the other hand, self-propagating combustion was achieved for all stoichiometries of the Cr_2O_3 + 2Al + yB samples with y = 1–8, and the associated flame-front velocities were around tenfold higher than those of the Cr_2O_3–B samples. It is interesting to note that as revealed in Fig. 3, the variation of flame-front velocity of the Cr_2O_3–Al–B sample with molar ratio of B/Cr_2O_3 is in a similar manner to that exhibited by the Cr_2O_3–B sample. For the Al-added reactant compacts, the maximum flame-front velocity reaching 18.5 mm/s was observed under the boron content of y = 4. The composition dependence of the combustion velocity is generally in agreement with that of reaction exothermicity. The exothermicity of combustion synthesis could be complicated by different boride phases formed in the final product, the extent of metallothermic reduction involved in the overall reaction, and the dilution effect of excess boron.

3.3. Measurement of combustion temperature

The combustion temperature serves as a good indication of the reaction exothermicity. For the Cr_2O_3–B powder compacts, four temperature profiles depicted in Fig. 4 show an increase in the sample temperature as the combustion front approaches and a mild decrease after the passage of the reaction front. As far as the sample stoichiometry is concerned, the increase of the combustion front temperature from 675 to 830 °C is noticed in Fig. 4 with boron content from x = 4 to 6, followed by a decline as the amount of boron augments further.

In comparison with those observed for the Cr_2O_5–B samples, Fig. 5 reveals a steeper climb and the larger magnitude of the temperature for the Cr_2O_3–Al–B samples. The abrupt rise in temperature signifies the rapid arrival of the combustion front. The higher temperature is a consequence of the fact that the synthesis reaction involving Cr_2O_3 under aluminothermic reduction is more energetic than that subjected to borothermic reduction. As indicated in Fig. 5, with increasing boron from y = 1 to 8 the peak combustion

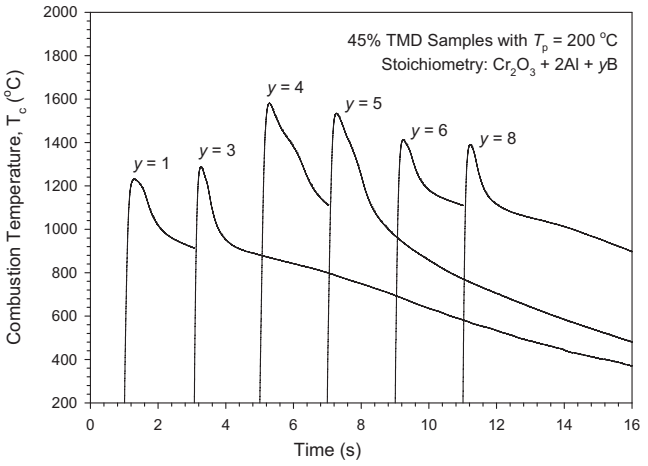

Fig. 5. Effect of boron content on combustion temperature of powder compacts with stoichiometry of Cr_2O_3 + 2Al + yB.

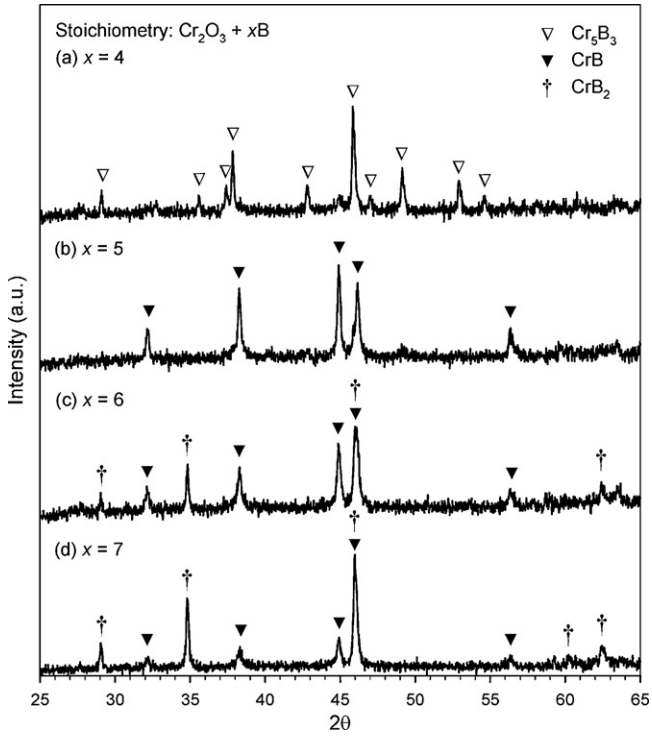

Fig. 6. XRD patterns of products synthesized from samples of $Cr_2O_3 + xB$ with (a) $x = 4$, (b) $x = 5$, (c) $x = 6$, and (d) $x = 7$.

temperature rises from about 1230 to 1580 °C at $y = 4$, after that a fall to 1390 °C is seen. Most importantly, the variation of combustion temperature with sample stoichiometry is in a manner consistent with that of flame-front velocity.

3.4. Phase constituents and morphology of synthesized products

Fig. 6(a)–(d) plots the XRD patterns of synthesized products from the Cr_2O_3–B samples. According to the XRD analysis, single-phase Cr_5B_3 and CrB were produced from the samples of $x = 4$ and 5, respectively. The reactant compacts with B/Cr_2O_3 = 6 and 7 yielded CrB–CrB_2 mixtures, within which the fraction of CrB_2 increases with molar ratio of B/Cr_2O_3. Further increase in boron, such as the stoichiometry of Cr_2O_3 + 9B, led to the formation of CrB_2 as the only boride phase in the end product. No detection of B_2O_3 by XRD is due probably to its glassy nature. Besides, previous studies [9,10,19] reported that the majority of B_2O_3 yielded from borothermic reduction of metal oxides could be evaporated or voluntarily expelled in the form of very tiny liquid droplets from the porous sample, thus resulting in the absence of B_2O_3 in the final product.

A list of chromium borides formed from the Cr_2O_3–B samples of different stoichiometries is presented in Table 1, indicating formation of three boride phases. Moreover, an additional quantity of boron was found to be required for the yield of boride compounds. For example, the sample with $x = 4$ produces Cr_5B_3 rather than CrB, which is the stoichiometric phase to be formed based upon reaction (1), while the sample with a molar proportion of Cr_2O_3:B = 1:5 favors the formation

Table 1
Summary of phase composition of synthesized products with respect to their initial stoichiometry of $Cr_2O_3 + xB$ samples.

Value of x in $Cr_2O_3 + xB$	Phase composition of synthesized products	
	Dominant boride	Secondary boride
4	Cr_5B_3	
4.67	CrB	Cr_5B_3
5	CrB	
6	CrB	CrB_2
7, 8	CrB_2	CrB
9	CrB_2	

of CrB. The need of an excess amount of boron is partly to compensate the relatively low purity of amorphous boron about 92%, and in part to account for the loss of boron due to evaporation during the SHS process. According to Peshev et al. [17], the loss of boron as BO in the borothermic reduction of Cr_2O_3 was responsible for the presence of a boron-deficient phase CrB along with CrB_2 in the final product. Here the absence of Cr_2B and CrB_4 resulted mainly from no combustion for the green compacts intended for their formation. Another compound Cr_3B_4 representing an intermediate phase between CrB and CrB_2 was not detected, implying that it is less stable to exist than CrB and CrB_2.

The XRD patterns depicted in Fig. 7(a)–(e) show phase constituents of the products synthesized from the Cr_2O_3–Al–B samples. The presence of Al_2O_3 confirms the role of Al as the key reducing agent of Cr_2O_3. Except CrB_4 there are five chromium borides identified in Fig. 7. Moreover, Fig. 7(a), (c),

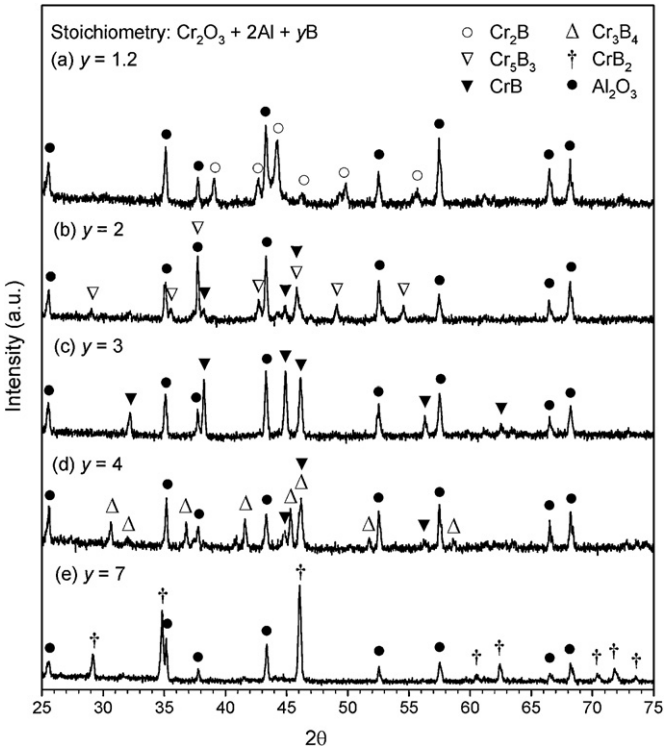

Fig. 7. XRD patterns of products synthesized from samples of $Cr_2O_3 + 2Al + yB$ with (a) $y = 1.2$, (b) $y = 2$, (c) $y = 3$, (d) $y = 4$, and (e) $y = 7$.

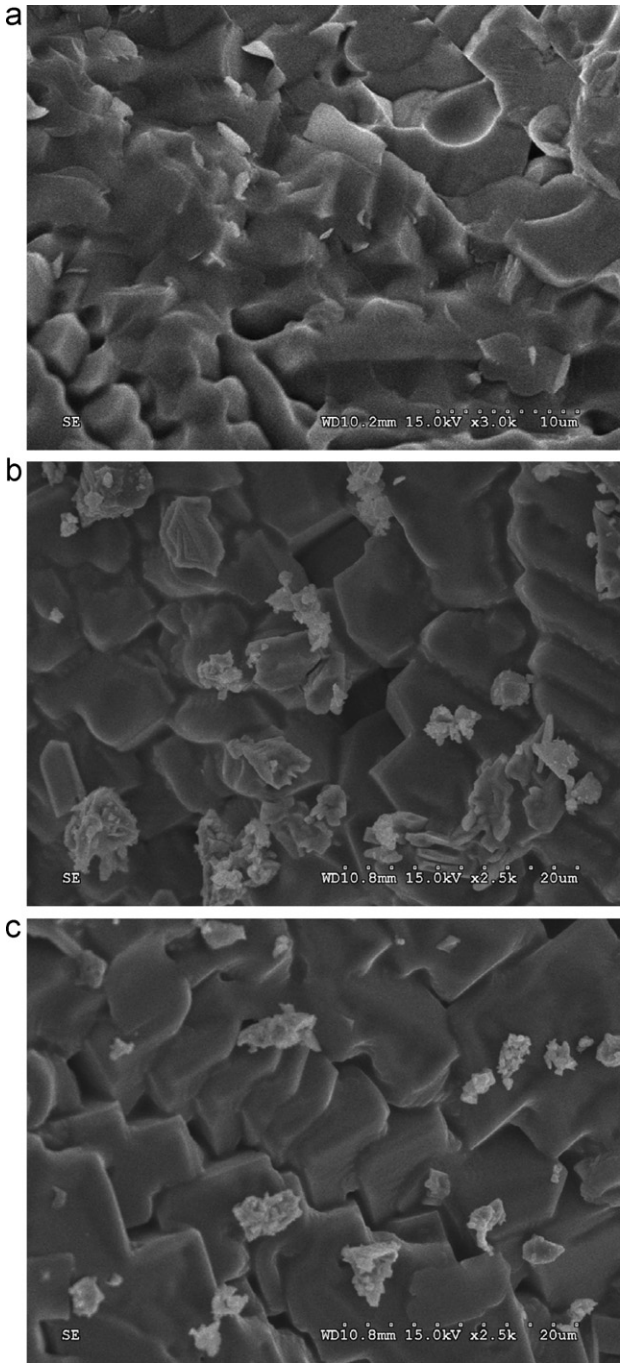

Fig. 8. SEM micrographs of fracture surfaces of products synthesized from samples of (a) Cr_2O_3:B = 1:8, (b) Cr_2O_3:Al:B = 1:2:3, and (c) Cr_2O_3:Al:B = 1:2:7.

and (e) indicates the yield of Cr_2B, CrB, and CrB_2 as the only boride phase from the green compacts with $y = 1.2$, 3, and 7, respectively. Table 2 summarizes the dominant and secondary borides formed in the final products with respect to their initial compositions. It was found that Cr_5B_3 and Cr_3B_4 were produced along with other borides and were recognized as the dominant boride in the cases of $y = 2$ and 4, as shown in Fig. 7(b) and (d). The presence of Cr_3B_4 implies that the SHS process of the Al-added sample is more favorable for the formation of complex or metastable phases, on account of its

Table 2
Summary of phase composition of synthesized products with respect to their initial stoichiometry of $Cr_2O_3 + 2Al + yB$ samples.

Value of y in $Cr_2O_3 + 2Al + yB$	Phase composition of synthesized products		
	Dominant boride	Secondary boride	Oxide
1.2	Cr_2B		Al_2O_3
1.5	Cr_2B	Cr_5B_3	Al_2O_3
2	Cr_5B_3	CrB	Al_2O_3
3	CrB		Al_2O_3
4	Cr_3B_4	CrB	Al_2O_3
5, 6	CrB_2	Cr_3B_4	Al_2O_3
7, 8	CrB_2		Al_2O_3

sharp thermal gradient and rapid cooling rate. In addition, excess boron was also required by the Cr_2O_3–Al–B samples to produce chromium borides. Therefore, the absence of CrB_4 could be due to a deficiency of boron or its limited existence range shown in Fig. 1.

Fig. 8(a)–(c) shows SEM micrographs of the fracture surface of synthesized products. The microstructure associated with the product fabricated from the sample of Cr_2O_3:B = 1:8 in Fig. 8(a) exhibits a mixed fracture mode with more of transgranular and less of intergranular. Boride grains of about 3–5 μm are likely to be formed from the melt. For the Al-added powder compacts of Cr_2O_3:Al:B = 1:2:3 and 1:2:7, Fig. 8(b) and (c) indicates an intergranular fracture. The grain size is about 8–12 μm and fine gaps of around 1–2 μm are visible at grain junctions. Generally speaking, the longer duration of synthesis for the Cr_2O_3–B sample could contribute a better particle bonding to the final product.

4. Conclusions

This study presents an investigation on the preparation of chromium borides through the SHS process involving borothermic and aluminothermic reduction of Cr_2O_3. In view of the existence of six chromium borides (Cr_2B, Cr_5B_3, CrB, Cr_3B_4, CrB_2, and CrB_4), the reactant mixtures were prepared with a broad range of the boron content.

Formation of chromium borides based upon borothermic reduction was conducted by adopting the samples of $Cr_2O_3 + xB$ with $x = 3$–10. However, self-sustaining combustion is feasible within a stoichiometric range of $4 \leq x \leq 9$. With the increase of the boron content, the temperature and velocity of the combustion front increased, reached their maxima of 830 °C and 2.56 mm/s at $x = 6$, and then decreased. Based upon characterization of the products by XRD, three boride phases Cr_5B_3, CrB, and CrB_2 in the monolithic form were produced from samples of $x = 4$, 5, and 9, respectively. They are also present as a CrB–Cr_5B_3 composite from the sample of $x = 4.67$ or a CrB–CrB_2 composite from samples of $x = 6$–8. It was found that an excess amount of boron was required for the formation of boride compounds.

For combustion synthesis involving aluminothermic reduction of Cr_2O_3, the powder compacts composed of $Cr_2O_3 + 2Al + yB$ with $y = 1$–8 were all combustible and Al_2O_3-added chromium borides were produced. On account of the greater

exothermicity for reduction of Cr_2O_3 by Al, the combustion temperature (1230–1580 °C) and flame-front velocity (7.6–18.5 mm/s) of the Cr_2O_3–Al–B samples are much higher than those of the Cr_2O_3–B samples. The XRD patterns identify the formation of five chromium borides in the Al_2O_3-added products. Among them, Cr_2B, CrB, and CrB_2 are present as the sole boride compound in the cases of $y = 1.2$, 3, and 7 or 8, respectively; Cr_5B_3 and Cr_3B_4, were synthesized along with CrB as the minor phase from the corresponding samples of $y = 2$ and 4. Likewise, the Cr_2O_3–Al–B reactant compact needs boron in excess of the stoichiometric amount to produce chromium borides.

Acknowledgment

This research was sponsored by the National Science Council of Taiwan, ROC, under the grants of NSC 100-2221-E-035-074-MY2.

References

[1] R. Telle, Boride and carbide ceramics, in: M.V. Swain (Ed.), Structure and Properties of Ceramics, Materials Science and Technology, vol. 11, Wiley-VCH, Weinheim, 2005.
[2] W.G. Fahrenholtz, G.E. Hilmas, I.G. Talmy, J.A. Zaykoski, Refractory diborides of zirconium and hafnium, Journal of the American Ceramic Society 90 (5) (2007) 1347–1364.
[3] I.P. Borovinskaya, A.G. Merzhanov, N.P. Novikov, A.K. Filonenko, Gasless combustion of mixtures of powdered transition metals with boron, Combustion Explosion and Shock Waves 10 (1974) 2–10.
[4] J. Wong, E.M. Larson, P.A. Waide, R. Frahm, Combustion front dynamics in the combustion synthesis of refractory metal carbides and diborides using time-resolved X-ray diffraction, Journal of Synchrontron Radiation 13 (2006) 326–335.
[5] H.E. Çamurlu, F. Maglia, Preparation of nano-size ZrB_2 powder by self-propagating high-temperature synthesis, Journal of the European Ceramic Society 29 (2009) 1501–1506.
[6] C.L. Yeh, H.J. Wang, Combustion synthesis of vanadium borides, Journal of Alloys and Compounds 509 (2011) 3257–3261.
[7] C.L. Yeh, H.J. Wang, A comparative study on combustion synthesis of Ta–B compounds, Ceramics International 37 (2011) 1569–1573.
[8] Z.A. Munir, U. Anselmi-Tamburini, Self-propagating exothermic reactions: the synthesis of high-temperature materials by combustion, Materials Science Reports 3 (1989) 277–365.
[9] C.L. Yeh, W.S. Hsu, Preparation of molybdenum borides by combustion synthesis involving solid-phase displacement reactions, Journal of Alloys and Compounds 457 (2008) 191–197.
[10] C.L. Yeh, H.J. Wang, Preparation of tungsten borides by combustion synthesis involving borothermic reduction of WO_3, Ceramics International 37 (2011) 2597–2601.
[11] T.B. Massalski, H. Okamoto, P.R. Subramanian, L. Kacprzak (Eds.), Binary Alloy Phase Diagrams, ASM International, Materials Park, OH, USA, 1996.
[12] M. Audronis, A. Leyland, P.J. Kelly, A. Matthews, The effect of pulsed magnetron sputtering on structure and mechanical properties of CrB_2 coatings, Surface and Coatings Technology 201 (2006) 3970–3976.
[13] L.R. Jordan, A.J. Betts, K.L. Dahm, P.A. Dearnley, G.A. Wright, Corrosion and passivation mechanism of chromium diboride coatings on stainless steel, Corrosion Science 47 (2005) 1085–1096.
[14] D. Radev, Z. Zahariev, Oxidation stability of B_4C–Me_xB_y composite materials, Journal of Alloys and Compounds 197 (1993) 87–90.
[15] S. Yamada, K. Hirao, Y. Yamauchi, S. Kanzaki, Mechanical and electrical properties of B_4C–CrB_2 ceramics fabricated by liquid phase sintering, Ceramics International 29 (2003) 299–304.
[16] K. Iizumi, K. Kudaka, D. Maezawa, T. Sasaki, Mechanochemical synthesis of chromium borides, Journal of the Ceramic Society of Japan 107 (1999) 491–493.
[17] P. Peshev, G. Bliznakov, L. Leyarovska, On the preparation of some chromium, molybdenum and tungsten borides, Journal of the Less-Common Metals 13 (1967) 241–247.
[18] C.L. Yeh, H.J. Wang, Preparation of borides in Nb–B and Cr–B systems by combustion synthesis involving borothermic reduction of Nb_2O_5 and Cr_2O_3, Journal of Alloys and Compounds 490 (2010) 366–371.
[19] J.K. Sonber, T.S.R.Ch. Murthy, C. Subramanian, S. Kumar, R.K. Fotedar, A.K. Suri, Investigation on synthesis, pressureless sintering and hot pressing of chromium diboride, International Journal of Refractory Metals and Hard Materials 27 (2009) 912–918.
[20] A.G. Merzhanov, Combustion processes that synthesize materials, Journal of Materials Processing Technology 56 (1996) 222–241.
[21] D. Vallauri, V.A. Shcherbakov, A.V. Khitev, F.A. Deorsola, Study of structure formation in TiC–TiB_2–Me_xO_y ceramics fabricated by SHS and densification, Acta Materialia 56 (2008) 1380–1389.
[22] D. Horvitz, I. Gotman, E.Y. Gutmanas, N. Glaussen, In situ processing of dense Al_2O_3–Ti aluminide interpenetrating phase composites, Journal of the European Ceramic Society 22 (2002) 947–954.
[23] S.K. Mishra, S.K. Das, V. Sherbacov, Fabrication of Al_2O_3–ZrB_2 in situ composite by SHS dynamic compaction: a novel approach, Composites Science and Technology 67 (2007) 2447–2453.
[24] Q. Hu, P. Luo, Y. Yan, Microstructures, densification and mechanical properties of TiC–Al_2O_3–Al composite by field-activated combustion synthesis, Materials Science and Engineering A 486 (2008) 215–221.
[25] M. Gu, C. Huang, S. Xiao, H. Liu, Improvements in mechanical properties of TiB_2 ceramics tool materials by dispersion of Al_2O_3 particles, Materials Science and Engineering A 486 (2008) 167–170.
[26] A.R. Keller, M. Zhou, Effect of microstructure on dynamic failure resistance of titanium diboride/alumina ceramics, Journal of the American Ceramic Society 86 (3) (2003) 449–457.
[27] C.L. Yeh, Y.L. Chen, An experimental study on self-propagating high-temperature synthesis in the Ta–B_4C System, Journal of Alloys and Compounds 478 (2009) 163–167.
[28] M. Binnewies, E. Milke, Thermochemical Data of Elements and Compounds, Wiley-VCH Verlag GmbH, Weinheim/New York, 2002.